Human Reproduction, pp. 1–11, 2022
https://doi.org/10.1093/humrep/deac016

human reproduction

ORIGINAL ARTICLE *Embryology*

Fluorescence lifetime imaging microscopy (FLIM) detects differences in metabolic signatures between euploid and aneuploid human blastocysts

Jaimin S. Shah [1,2,3], Marta Venturas [4,5], Tim H. Sanchez, Alan S. Penzias[1,2,3], Daniel J. Needleman[4,6,†], and Denny Sakkas [3,*,†]

[1]Department of Obstetrics and Gynecology, Beth Israel Deaconess Medical Center, Boston, MA, USA [2]Department of Obstetrics, Gynecology and Reproductive Biology, Harvard Medical School, Boston, MA, USA [3]Boston IVF, Waltham, MA, USA [4]Molecular and Cellular Biology and School of Engineering and Applied Sciences, Harvard University, Cambridge, MA, USA [5]Department de Biologia Cel.lular, Fisiologia i Immunologia, Universitat Autònoma de Barcelona, Cerdanyola, Spain [6]Center for Computational Biology, Flatiron Institute, New York, NY, USA

*Correspondence address. Boston IVF, 130 Second Avenue, Waltham, MA 02451, USA. Tel: 781-370-2325;
E-mail: dsakkas@bostonivf.com https://orcid.org/0000-0002-9509-6791

Submitted on September 03, 2021; resubmitted on December 29, 2021; editorial decision on January 14, 2022

STUDY QUESTION: Can non-invasive imaging with fluorescence lifetime imaging microscopy (FLIM) detect metabolic differences in euploid versus aneuploid human blastocysts?

SUMMARY ANSWER: FLIM has identified significant metabolic differences between euploid and aneuploid blastocysts.

WHAT IS KNOWN ALREADY: Prior studies have demonstrated that FLIM can detect metabolic differences in mouse oocytes and embryos and in discarded human blastocysts.

STUDY DESIGN, SIZE, DURATION: This was a prospective observational study from August 2019 to February 2020. Embryo metabolic state was assessed using FLIM to measure the autofluorescence metabolic factors nicotinamide adenine dinucleotide dehydrogenase together with nicotinamide adenine phosphate dinucleotide dehydrogenase (NAD(P)H) and flavin adenine dinucleotide (FAD). Eight metabolic FLIM parameters were obtained from each blastocyst (four for NAD(P)H and four for FAD): short (T_1) and long (T_2) fluorescence lifetime, fluorescence intensity (*I*) and fraction of the molecules engaged with enzymes (*F*). The redox ratio (NAD(P)H-*I*)/(FAD-*I*) was also calculated for each image.

PARTICIPANTS/MATERIALS, SETTING, METHODS: This study was performed at a single academically affiliated centre where there were 156 discarded frozen blastocysts (n = 17 euploids; 139 aneuploids) included. Ploidy status was determined by pre-implantation genetic testing for aneuploidy (PGT-A). Discarded human blastocysts were compared using single FLIM parameters. Additionally, inner cell mass (ICM) and trophectoderm (TE) were also evaluated. Multilevel models were used for analysis. A post-hoc correction used Benjamini–Hochberg's false discovery rate, at a *q*-value of 0.05.

MAIN RESULTS AND THE ROLE OF CHANCE: Comparing euploid (n = 17) versus aneuploid (n = 139) embryos, a significant difference was seen in NAD(P)H-*F* ($P < 0.04$), FAD-*I* ($P < 0.04$) and redox ratio ($P < 0.05$). Euploid ICM (n = 15) versus aneuploid ICM (n = 119) also demonstrated significantly different signatures in NAD(P)H-*F* ($P < 0.009$), FAD-*I* ($P < 0.03$) and redox ratio ($P < 0.03$). Similarly, euploid TE (n = 15) versus aneuploid TE (n = 119) had significant differences in NAD(P)H-*F* ($P < 0.0001$) and FAD-*I* ($P < 0.04$).

LIMITATIONS, REASONS FOR CAUTION: This study utilized discarded human blastocysts, and these embryos may differ metabolically from non-discarded human embryos. The blastocysts analysed were vitrified after PGT-A biopsy and it is unclear how the vitrification process may affect the metabolic profile of blastocysts. Our study was also limited by the small number of rare donated euploid embryos

[†]These authors contributed equally to this study.

available for analysis. Euploid embryos are very rarely discarded due to their value to patients trying to conceive, which limits their use for research purposes. However, we controlled for the imbalance with the bootstrap resampling analysis.

WIDER IMPLICATIONS OF THE FINDINGS: These findings provide preliminary evidence that FLIM may be a useful non-invasive clinical tool to assist in identifying the ploidy status of embryos.

STUDY FUNDING/COMPETING INTEREST(S): The study was supported by the Blavatnik Biomedical Accelerator Grant at Harvard University. Becker and Hickl GmbH and Boston Electronics sponsored research with the loaning of equipment for FLIM. D.J.N. is an inventor on patent US20170039415A1. There are no other conflicts of interest to declare.

TRIAL REGISTRATION NUMBER: N/A

Key words: fluorescence lifetime imaging microscopy / FLIM / mitochondria / euploid / aneuploid

Introduction

Optimizing embryo selection to improve ART outcome is a central objective in ART. The most widely used selection criterion has been the grading system based on embryo morphology. With the worldwide trend to culture embryos to the blastocyst stage, the use of an alphanumeric scoring system evaluating blastocyst expansion, inner cell mass (ICM) and trophectoderm (TE) to grade blastocysts is widely used (Schoolcraft *et al.*, 1999). Prior studies have shown correlations in blastocyst morphology with implantation and live birth (Gardner *et al.*, 2000a; Ahlström *et al.*, 2011; Van Den Abbeel et al., 2013) but the relative contributions of the ICM and TE are still disputed (Hill *et al.*, 2013; Irani *et al.*, 2017). Thus, morphological embryo assessment is accepted to be helpful, but it has well-known limitations (Wong *et al.*, 2014). A number of studies have also shown that euploid blastocysts with varying morphology had similar implantation rates (Capalbo *et al.*, 2014; Shear *et al.*, 2020). Even embryos with deviant morphology and suboptimal morphokinetics of embryo development may still result in a live birth (Stecher *et al.*, 2014). One parameter that has been shown to distinguish embryos with the same morphological scores is metabolism (Gardner *et al.*, 2011), suggesting that morphology is not clearly connected to the underlying biochemical variables necessary for embryo viability (Gardner *et al.*, 2000b). Furthermore, prior studies have measured the oxygen consumption rate in pre-implantation blastocyst development to better understand the changes in mitochondrial function (Hashimoto *et al.*, 2017; Muller *et al.*, 2019).

A number of innovations in ART pertaining to embryo selection have shown some promise but have not yet demonstrated clinical utility. Time-lapse imaging with conventional light microscopy can be used to record the dynamics of cleavage and changes in embryo morphology. Prior studies have shown limited evidence of a clinical benefit with time-lapse imaging (Armstrong *et al.*, 2015; Goodman *et al.*, 2016; Yang *et al.*, 2018). There has previously been great excitement about the potential to combine time-lapse with artificial intelligence to improve embryo selection (Fernandez et al., 2020). Some approaches attempt to develop 'black-box' predictions of embryo quality (Simopoulou *et al.*, 2018; VerMilyea *et al.*, 2020), while others seek to automatically extract biologically and clinically interpretable information from the time-lapse movies (Leahy *et al.*, 2020). While the use of artificial intelligence to aid embryo selection shows promise (Tran *et al.*, 2019; VerMilyea *et al.*, 2020), there are both practical and ethical issues that need to be addressed before such methods can be responsibly made part of clinic treatment (Afnan *et al.*, 2021). Other black-box approaches included metabolomic assessment of embryo culture media using near-infrared spectroscopy as an indicator of embryo viability (Hardarson *et al.*, 2012; Vergouw *et al.*, 2012). The failure of this method in randomized trials provided a warning of the difficulty in translating these methodologies to the clinic.

Pre-implantation genetic testing for aneuploidy (PGT-A) by TE biopsy has been advocated for aiding in embryo selection by determining the ploidy status of an embryo. While some studies of PGT-A have shown increased pregnancy rates (Scott *et al.*, 2013) mainly in older patients (Munné *et al.*, 2019; Murphy *et al.*, 2019), there are numerous mitigating factors worthy of consideration, including cost, the invasive nature of TE biopsy, differences in PGT-A rates among clinics and copy number variant (mosaicism) interpretation (Capalbo *et al.*, 2016; Practice Committees of the American Society for Reproductive Medicine and the Society for Assisted Reproductive Technology, 2018; Practice Committee and Genetic Counseling Professional Group (GCPG) of the American Society for Reproductive Medicine, 2020). PGT-A has provided numerous lessons in over-interpreting embryo analysis. Numerous studies have shown that the TE biopsy may or may not always accurately represent the status of the whole embryo (Chuang *et al.*, 2018; Popovic *et al.*, 2019; Victor *et al.*, 2019). Of greatest concern, however, is the fact that blastocysts diagnosed as mosaic, which could potentially be discarded, have been shown to be viable (Capalbo *et al.*, 2021). In addition, there are still up to 40% of euploid embryos that fail to implant (Scott *et al.*, 2013) possibly due to other non-genetic factors or metabolic dysfunction. The development of non-invasive PGT-A (niPGT-A) to analyse conditioned blastocyst culture media may help alleviate the need for an invasive TE biopsy and may cost less (Rubio *et al.*, 2020). Proponents of niPGT-A and artificial intelligence scores of embryos are arguing that ranking of embryos could be a better approach so that the possibility of discarding viable embryos is drastically reduced. In reality, this approach would be the most beneficial and was originally proposed in other metabolic assessment technologies (Seli *et al.*, 2010).

Non-invasive metabolic imaging that measures cellular metabolism has been used in many fields (Becker, 2012), but its use in reproductive biology is limited. A prior study used non-invasive optical imaging by hyperspectral microscopy and detected variance in metabolic activity by ploidy status in a mouse model (Tan *et al.*, 2020) and by the influence of oxygen levels *in vitro* in a bovine model (Sutton-Mcdowall *et al.*, 2017). Another non-invasive imaging modality, fluorescence lifetime imaging microscopy (FLIM) was able to detect metabolic differences in mouse oocytes (Sanchez *et al.*, 2018) and embryos (Ma *et al.*, 2019; Sanchez *et al.*, 2019; Seidler et al., 2020). Furthermore, one

study utilizing FLIM was able to show intricate metabolic differences in human blastocysts when comparing their day of development, embryo expansion stage, ICM and TE (Venturas *et al.*, 2022).

Given the promising FLIM results from prior mouse model and discarded human blastocyst studies, continued exploration of this technology is warranted to see if it can aid in embryo selection. The purpose of our study was to investigate whether non-invasive FLIM can detect metabolic differences between euploid and aneuploid human blastocysts. Additionally, we explored these metabolic differences within the ICM and TE separately.

Materials and methods

This was a prospective observational study at a single academically affiliated centre from August 2019 to February 2020. Human blastocysts were discarded and donated for research under determinations by the Beth Israel Deaconess Medical Center and New England institutional review boards (New England IRB WO 1-6450-1). Ploidy status (euploid versus aneuploid) for all embryos were determined by PGT-A using next-generation sequencing from a TE biopsy followed by immediate vitrification. Embryos were deemed euploid or aneuploid, and embryonic mosaicism data were not reported. The majority of embryos were either Day 5 or 6 with only four embryos that were Day 7 and were of Schoolcraft and Gardner (Schoolcraft *et al.*, 1999) morphology grade A or B except three embryos which were Grade C. Morphology and expansion assessment were performed prior to vitrification.

All discarded vitrified blastocysts were warmed and cultured for 2 h in individual drops of 50 µl of continuous single culture complete media with human serum albumin media overlain with mineral oil in an incubator at 37°C, 7% CO_2 and 6% O_2 prior to collecting images with FLIM. Blastocysts were vitrified and warmed using the FUJIFILM Irvine Scientific vitrification system (Santa Ana, CA, USA). Once embryos were warmed and expanded, embryos were transferred into a custom glass-bottom microwell dish with 80 µl of culture media overlain with mineral oil and imaged. The FLIM on-stage incubation system (Ibidi GmbH, Martinsried, Germany) was temperature controlled (37°C) and set at 7% CO_2 and 6% O_2 to maintain culture conditions while imaging.

Fluorescence lifetime imaging microscopy

FLIM measurements were performed on a Nikon TE300 (Nikon, Japan) microscope using two-photon excitation from a Ti:Sapphire pulsed laser (M-squared Lasers, UK) with an 80 MHz repetition rate and 150 fs pulse width, a Galvo scanner that reflected the laser into the sample plane and scanned the focal point across the imaging field of view, time-correlated single-photon counting module (SPC-150, Becker and Hickl, Germany), and a hybrid single-photon counting detector (HPM-100-40, Becker and Hickl, Germany). Imaging was performed using a 20X Nikon objective with 0.75 numerical aperture (CFI Apo 20X, NA 0.75, Nikon). The fluorescence spectra of nicotinamide adenine dinucleotide dehydrogenase (NADH) and nicotinamide adenine phosphate dinucleotide dehydrogenase (NAD(P)H) are almost indistinguishable, and the resulting fluorescence combined from these two molecules is often referred to as the NAD(P)H signal (Ghukasyan and Heikal, 2014). An optical bandpass filter of 447/60 nm for (NAD(P)H) (BrightLine, Semrock, USA) and 550/88 nm for flavin adenine dinucleotide (FAD; Chroma technologies) was positioned in a filter wheel in front of the detector and an additional 650 nm short pass filter was mounted on the detector (Chroma Technology Corp., Bellow Falls, VT, USA). The laser excitation wavelengths for NAD(P)H and FAD imaging were set to 750 and 890 nm, respectively. The powers measured at the objective used were 12 mW for NAD(P)H and 20 mW for FAD and they were measured at the sample plane. Each NAD(P)H and FAD image was acquired with 60 s of scanning integration time. For each blastocyst, the ICM was identified and three Z-planes, seven microns apart were acquired using a customized motorized stage (CONEX TRA12CC actuators, Newport, USA). The ICM and TE of each Z-plane were manually segmented and were used for a portion of the analysis. All of the electronics were controlled by SPCM software (Becker and Hickl, Germany) and custom LabVIEW software.

Data analysis

Data were analysed using custom code in MATLAB version R2019b (MathWorks, USA). Supervised machine learning (Illastik, version 1.0) was used to segment intracellular versus background NAD(P)H and FAD intensity images of blastocysts. The algorithm was trained using 40 NAD(P)H and FAD intensity images. For each segment region, the photon arrival time histogram was fit assuming a two-exponential decay model:

$$P(t) = A[(1 - F * e^{(-t/\tau_1)}) + (F * e^{(-t/\tau_2)})] + B,$$

where A is a normalization factor, B is the background, τ_1 is the short lifetime, τ_2 is the long lifetime and F is the fraction of molecule with long lifetime (fraction engaged with enzymes for NAD(P)H and unengaged for FAD). We convolved this function with a measured instrument response function to model the experimental data and then performed a least-square fit that yielded quantitative values for these parameters. Eight metabolic parameters were obtained from each blastocyst (four for NAD(P)H and four for FAD): fluorescence intensity, short and long lifetimes, and fraction of the molecules engaged with enzymes. We calculated the fluorescence intensity for each embryo by dividing the number of photons by the area of the embryo and number of integrated scans. The redox ratio (NAD(P)H intensity)/(FAD intensity) was also calculated for each image.

Statistical analysis

We used Stata Statistical Software version 16.0 (LLC Stata Corp, College Station, TX, USA) to perform all statistical analyses. R Studio Version 1.3.959 (R Foundation for Statistical Computing, Vienna, Austria) was used to plot the results. Our data have a hierarchical structure, three images per embryo and one to seven embryos per patient. For this reason, we used multilevel models (Snijder and Bosker, 2011) to analyse our data. A post-hoc correction using Benjamini–Hochberg's false discovery rate (FDR), at a q-value of 0.05. FDR P-values <0.05 was considered significant. We also used a bootstrap resampling method to further investigate the statistical significance of our results: we iteratively resampled the dataset, with 100 draws and 100 repeats. We performed additional analysis to control

for the imbalance in the number of euploid and aneuploid embryos: we reran each test with a subset of the data consisting of 17 euploid embryos and 17 randomly selected aneuploid embryos. We then repeated this analysis 30 times and calculated the percentage of times that FLIM parameters showed significant association with the ploidy status of the embryo. A prior study that included the embryos in this cohort and non-PGT-A embryos found significant metabolic differences in the day of blastocyst development after fertilization and in the stage of blastocyst expansion but not in morphology (Venturas *et al.*, 2022). We controlled for day of blastocyst development, stage of blastocyst expansion, morphology and maternal age by having these as covariates in the multilevel modelling.

Results

There were 156 discarded blastocysts of known ploidy included from 110 patients. The mean maternal age (±SD) was 36 ± 4 years and mean (±SD) body mass index (kg/m^2) was 26 ± 5. Figure 1 shows sample blastocyst images collected with FLIM showing the intensity autofluorescence and the segmentation of the ICM and TE. While present in the cytoplasm, NAD(P)H is more highly concentrated in the mitochondria. FAD is almost exclusively localized to the mitochondria. Hence it is the heterogeneous spatial distribution of the mitochondria within the cells and between cells that leads to the visually apparent differences in fluorescence intensity. In Sanchez *et al.* (2019), their second figure, both the co-localization of NADH/FAD with mitochondria and the heterogeneity of mitochondria within the cells were demonstrated using a mitochondrial-specific fluorescence label, mitotracker. Mitochondrial clustering is a common feature in cells and sometimes occurs around the perinuclear region. However, we observe a notably lower fluorescence signal within the nuclei, as NAD(P)H and FAD are excluded from the nucleus (Venturas *et al.*, 2022). We do not observe an apparent difference between the intensities of the ICM and the TE. There is unidentified punta in some of the cells that fluoresce strongly in the FAD fluorescence channel. They do not appear to be mitochondrial signal but may also contribute to the apparent clustering of the fluorescent signal in some regions.

When comparing euploid (n = 17) versus aneuploid (n = 139) blastocysts, significant differences were was seen in the NAD(P)H fraction engaged ($P < 0.04$), the FAD intensity ($P < 0.04$) and the redox ratio ($P < 0.05$; Fig. 2). NAD(P)H fraction engaged was still significant when

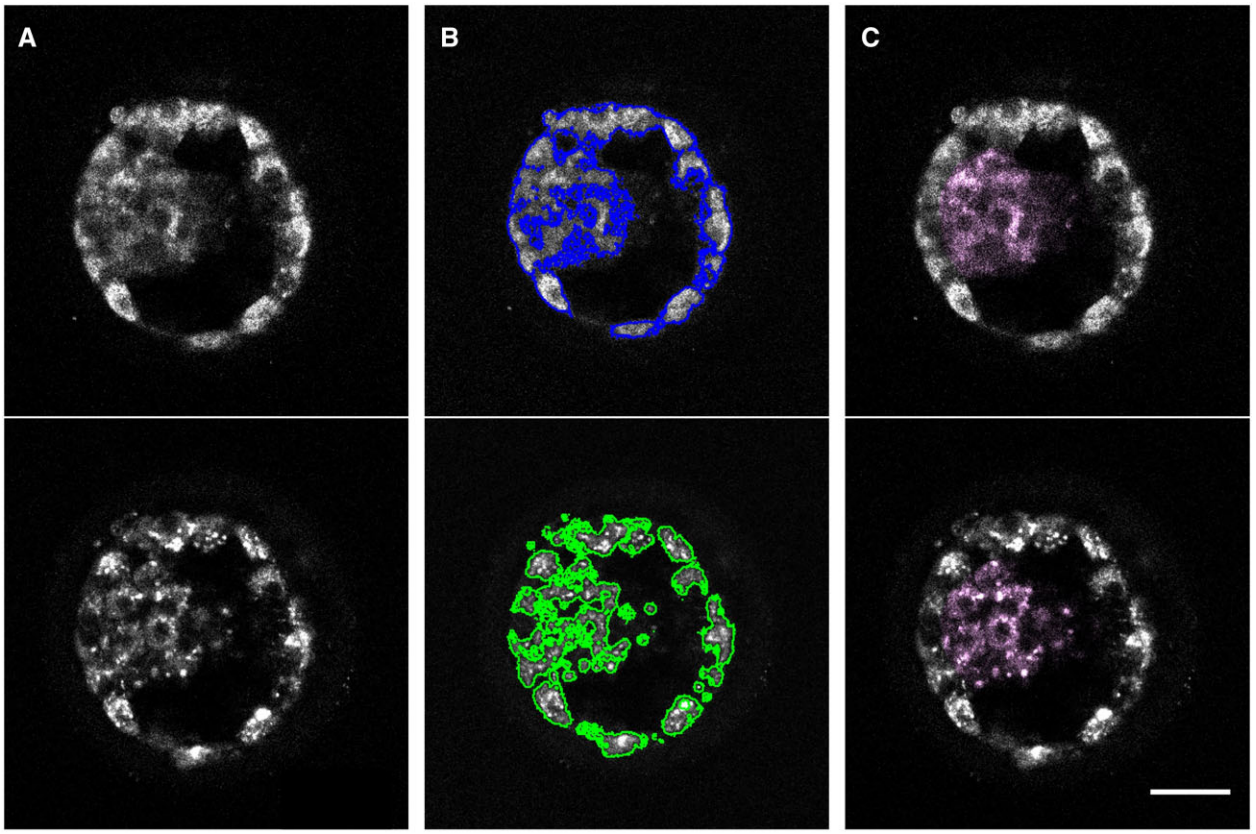

Figure 1. Sample images of human blastocysts using FLIM. (**a**) Sample blastocyst FLIM images showing intensity of NAD(P)H (top) and FAD (bottom); (**b**) machine learning-based segmented regions for analysis; (**c**) manual segmentation of the inner cell mass (magenta) and the trophectoderm (grey). The white line in the bottom right image represents 40 μm. FAD, flavin adenine dinucleotide; FLIM, fluorescence lifetime imaging microscopy; NAD(P)H, nicotinamide adenine phosphate dinucleotide dehydrogenase.

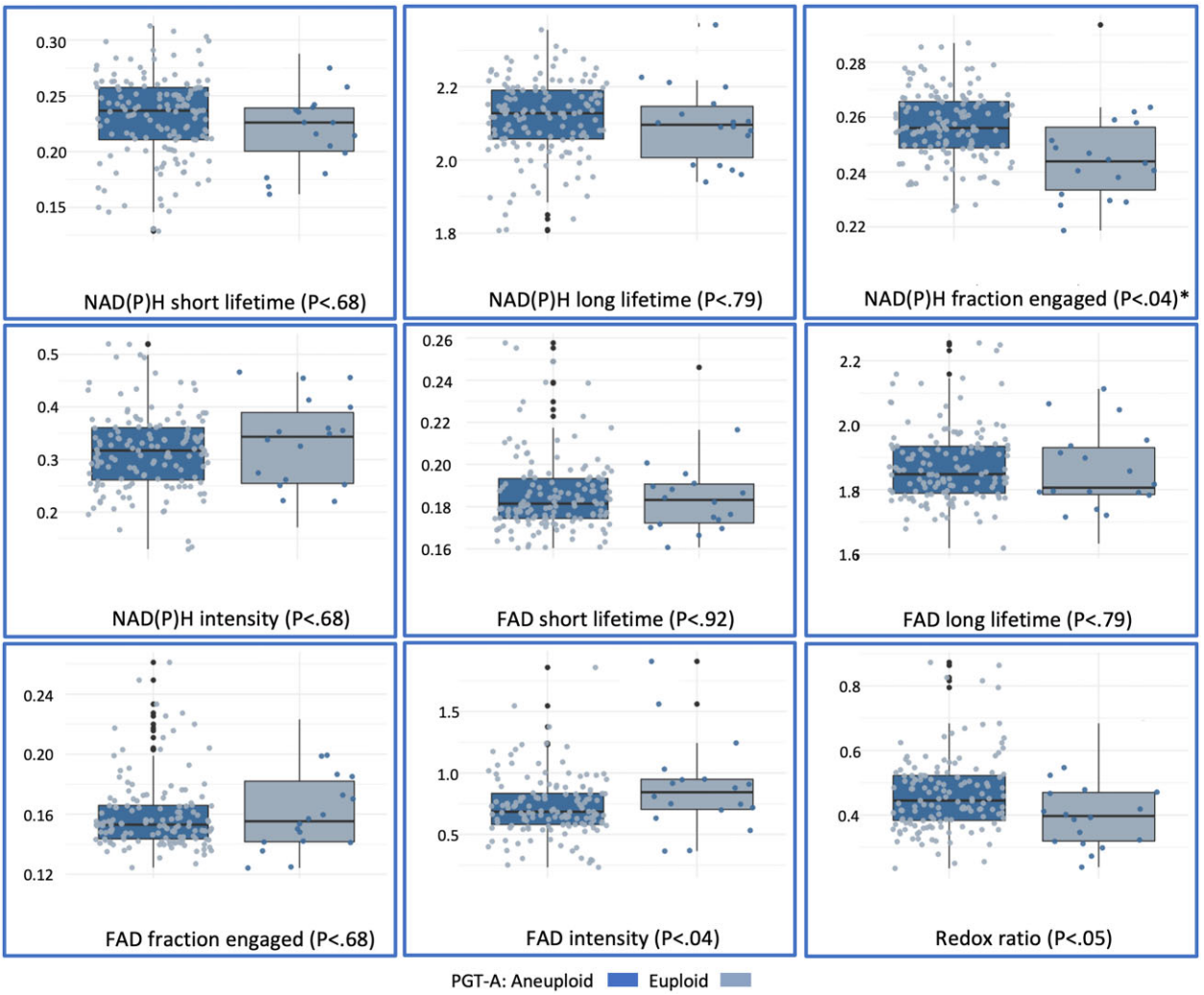

Figure 2. FLIM parameters, comparing euploid and aneuploid blastocysts. Adjusted variables: day of blastocyst development, stage of blastocyst expansion, morphology and maternal age. FLIM, fluorescence lifetime imaging microscopy. * represents statistical significance ($P < 0.05$).

controlling for the day of blastocyst development and the expansion stage. To further validate these results, we performed bootstrap resampling and found that these significant associations were upheld. To account for the imbalance in the number of euploid and aneuploid embryos, we reran this analysis using a subset of 17 aneuploid embryos chosen at random (i.e. equal in number to the euploid embryos). This analysis was repeated 30 times and we found significant associations 70% of the time with NAD(P)H fraction engaged, 30% of the time with FAD intensity and 13% of the time with redox ratio (and no significant associations with the other FLIM parameters).

Comparing euploid ICM (n = 15) versus aneuploid ICM (n = 119) also revealed statistically significant differences in the NAD(P)H fraction engaged ($P < 0.009$), the FAD intensity ($P < 0.03$) and the redox ratio ($P < 0.03$; Fig. 3). There were fewer embryos for this part of the analysis due to an inability to clearly manually segment the ICM in 22 embryos.

Figure 4 shows the comparison of euploid TE (n = 15) versus aneuploid TE (n = 119). This comparison similarly revealed statistically significant differences in the NAD(P)H fraction engaged ($P < 0.0001$) and FAD intensity ($P < 0.04$). To be consistent with the ICM analysis above, the same cohort of embryos was used for the TE analysis.

When comparing embryo biological sex, there were no statically significant differences observed in any FLIM parameters between male (n = 82) and female (n = 74) embryos. Similarly, no differences were seen in any FLIM parameter when comparing embryo sex for euploid or aneuploid embryos.

A sub-analysis was performed of the aneuploid blastocysts by specific chromosomal abnormality (any monosomy/trisomy (n = 88), chaotic (n = 33), triploidy (n = 12) and autosomal monosomy (n = 6)). Supplementary Table SI shows a breakdown of the types of aneuploidies. These specific aneuploidies were compared to euploid blastocysts (n = 17) and demonstrated a significant difference in the NAD(P)H fraction engaged ($P < 0.04$) and the FAD intensity ($P < 0.04$), with the

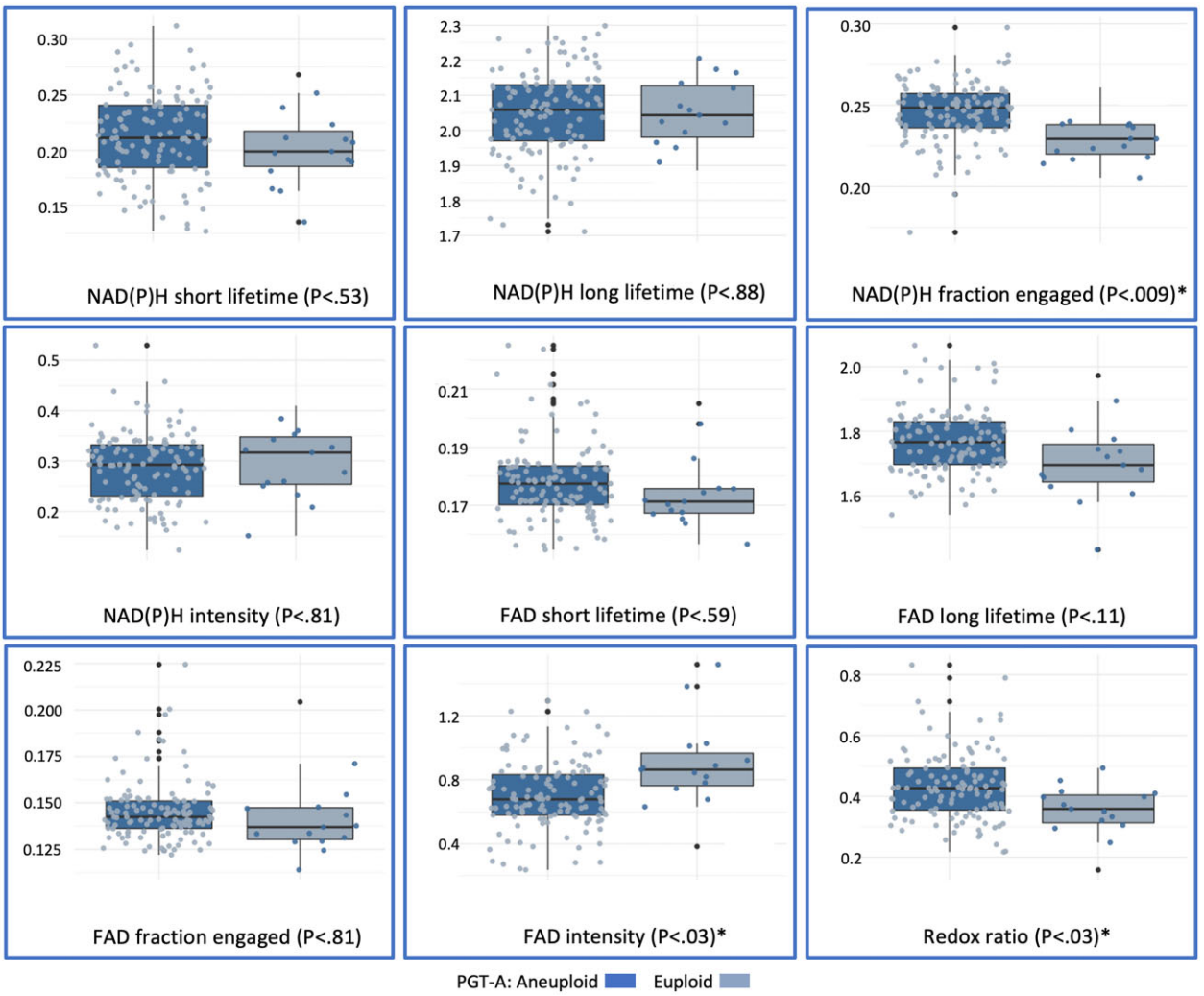

Figure 3. Inner cell mass (ICM) FLIM parameters, comparing euploid and aneuploid blastocysts. Adjusted variables: day of blastocyst development, stage of blastocyst expansion, morphology and maternal age. FLIM, fluorescence lifetime imaging microscopy. * represents statistical significance ($P < 0.05$).

redox ratio approaching significance ($P < 0.09$). When looking further at the NAD(P)H fraction engaged in the comparison of euploidy with each specific aneuploidy, only euploid versus any monosomy/trisomy showed a significant difference ($P < 0.02$) while euploid versus each other aneuploidy did not show a difference. There were no significant differences for FAD intensity and redox ratio when comparing euploidy with each specific aneuploidy. Comparing only between different aneuploidies showed no significant differences amongst the specific aneuploidy groups.

Discussion

In this prospective observational study, the use of non-invasive FLIM has shown quantitative metabolic differences between euploid and aneuploid embryos. Significant differences were detected with FLIM when signals of the embryo as a whole and the ICM and the TE of euploid blastocysts were compared to their aneuploid counterparts. These results show that metabolic differences detected with FLIM can provide further information on human blastocysts that might eventually aid in embryo selection.

Currently, the available options for embryo selection include morphology (non-invasive but subjective), PGT-A (objective with caveats but invasive) and niPGT-A (non-invasive and objective with caveats). PGT-A involves a technical procedure in which embryologists manipulate the blastocysts to obtain four to eight cells from an invasive TE biopsy. With this biopsy technique come specific challenges in that there may be variation of results from the same biopsy in different PGT-A laboratories as well as different PGT-A results from multiple biopsies of the same blastocyst, leading to the possibility of discarding normal blastocysts (Gleicher *et al.*, 2016; Patrizio *et al.*, 2019). Although there is an increasing amount of research on artificial intelligence and niPGT-

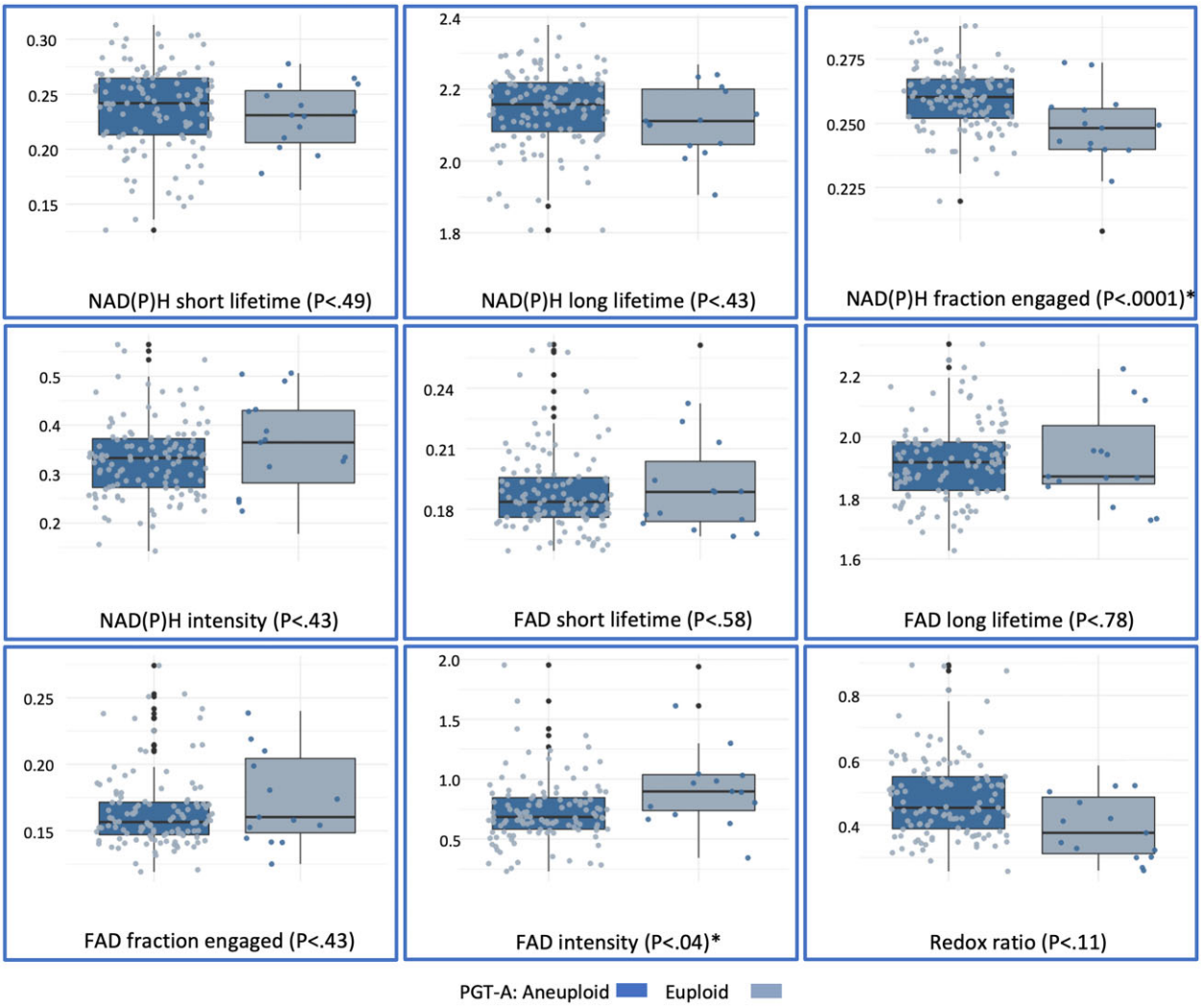

Figure 4. Trophectoderm (TE) FLIM parameters, comparing euploid and aneuploid blastocysts. Adjusted variables: day of blastocyst development, stage of blastocyst expansion, morphology and maternal age. FLIM, fluorescence lifetime imaging microscopy. * represents statistical significance ($P < 0.05$)

A, these technologies have not yet been demonstrated to be clinically useful (Simopoulou *et al.*, 2018; Tran *et al.*, 2019; Fernandez et al., 2020; Leahy *et al.*, 2020; Rubio *et al.*, 2020; VerMilyea *et al.*, 2020; Afnan *et al.*, 2021). FLIM offers another possible means to select embryos and provides information on metabolism which existing clinical technologies do not provide. FLIM, however, would not be a methodology to provide a definitive black and white delineation of viable and non-viable or euploid or aneuploid. We would expect that FLIM parameters would provide a ranking of the embryo cohort, to prioritize the order in which to transfer blastocysts. Previous studies have shown that FLIM can identify metabolic differences between normal mouse oocytes and those with metabolic dysfunction (Sanchez *et al.*, 2018), metabolic changes that occur during pre-implantation embryo development (Sanchez *et al.*, 2019) and metabolic response to oxygen deprivation in the mouse model (Seidler et al., 2020). Safety studies demonstrate that FLIM measurements do not significantly damage mouse embryos (Sanchez *et al.*, 2018, 2019). Furthermore, in the human model, FLIM has been able to detect metabolic differences in human blastocysts according to the day of development and expansion stage and identify the spatial pattern of the metabolic state between ICM and TE (Venturas *et al.*, 2022).

It has been reported that euploid and aneuploid blastocysts have different amounts of mitochondrial DNA (mtDNA; Ho *et al.*, 2018). mtDNA copy number has been found to be significantly elevated in aneuploid embryos versus euploid embryos (Diez-Juan *et al.*, 2015; Fragouli *et al.*, 2015), and this test has been touted as a possible clinical tool (Fragouli *et al.*, 2017). Euploid embryos that successfully implanted contained lower mtDNA quantities (Fragouli *et al.*, 2015). However, the utility of mtDNA is controversial and has fallen out of favour as a marker of embryo viability (Treff *et al.*, 2017). In contrast, the analysis of FLIM parameters in mouse oocyte models was shown to significantly improve the assessment of mitochondrial function when

compared to quantification of mtDNA copy number (Sanchez et al., 2018).

A number of other technologies have been shown to distinguish euploid and aneuploid embryos. These include the use of proteomics (McReynolds et al., 2011), mass spectrometry for distinct spectral pattern (Pais et al., 2020) and Raman Spectroscopy for footprint profiling (Liang et al., 2019) when analysing blastocyst culture media. In one such study, Pais et al. (2020) were able to show distinct spectral patterns for euploid and aneuploid genotypes in embryo culture media and identified 12 characteristic peak signatures for euploid and 17 peak signatures for aneuploid embryos. These data further highlight the hypothesis that chromosomal abnormalities can lead to different metabolic and proteomic signatures.

From our analysis, the NAD(P)H fraction engaged showed significant differences for all comparisons of euploid versus aneuploid embryos. Recent work has established a framework to relate NAD(P)H fraction engaged in oocytes to mitochondrial metabolic fluxes (Yang and Needleman, 2021) but it is unclear whether this is applicable to blastocysts. Changes in the NAD(P)H fraction engaged could arise from interactions with complex I in the mitochondria, enzymes in the tricarboxylic acid cycle, enzymes involved with glycolysis or the pentose phosphate pathway. The NAD(P)H fraction engaged was higher in aneuploid embryos than in euploid embryos in our study. It is unclear if this association is due to aneuploidy inducing metabolic defects, or, conversely, defects in metabolism causing aneuploidy. It has previously been proposed that embryo viability is associated with the amount of metabolic function, with healthy embryos being relatively 'quiet' (Leese, 2002). It is possible that aneuploid embryos have elevated metabolic processes giving them a more 'active' metabolism, leading to potentially increased levels of reactive oxygen species causing deleterious effects in the embryo (Leese et al., 2007). Other studies have also attempted to investigate the relationship between maternal age and mitochondrial functions in human embryos. For example, Morimoto et al. (2020) reported that mitochondrial function at the morula stage of human embryos decreased with maternal age and a decrease of mitochondrial function was also associated with a slow-paced development and impaired developmental rate from morula to blastocysts. Tao et al. (2017) also reported that mtDNA was significantly increased in aneuploid mouse embryos compared to euploid embryos. It remains to be answered whether our own measurements are a surrogate marker of ploidy status or whether ploidy defects directly influence mitochondrial activity.

In a prior study by Sanchez et al. (2019), they recorded metabolic measurements of mouse embryos with the FLIM every 2 h for 48 h at powers of 30 mW for NAD(P)H and 50 mW for FAD with 60 s of scanning integration time for three Z-planes which equated to 144 min of total imaging per embryo. There was no difference in birth rate or pup weight between the illuminated and control groups (Sanchez et al., 2019). However, in our study, our power was one-third (12mW for NAD(P)H and 20 mW for FAD) and each embryo was imaged for only 6 min which provides reassurance that there was no harm to the embryo.

Several limitations of this study need to be acknowledged. This study utilized discarded human blastocysts, and these embryos may differ metabolically from non-discarded human embryos. The PGT-A results from the TE biopsy may not be an accurate indicator of the presence or absence of aneuploid cells in the ICM. The designation of blastocysts as aneuploid or euploid may contain blastocysts with varying populations of euploid and aneuploid cells (Capalbo et al., 2021). How these relative ratios of euploid to aneuploid cells may influence FLIM parameters is at this stage unknown. Also, the blastocysts analysed were vitrified after PGT-A biopsy, thawed and warmed for 2 h prior to FLIM analysis. A prior study reported that the respiratory rate of vitrified blastocysts after warming was lower than in non-cryopreserved blastocysts but oxygen consumption of blastocysts with high developmental potential was restored earlier than in blastocysts with low developmental potential (Yamanaka et al., 2011). However, a prior study reported that vitrification does not alter mitochondrial potential or health (Nohales-Córcoles et al., 2016). Our study was limited by a small number of rare donated euploid embryos available for analysis. Euploid embryos are very rarely discarded due to their value to patients trying to conceive which limits their use for research purposes. However, we controlled for the imbalance with the bootstrap resampling analysis. An additional limitation is that aneuploid embryos may show both low and high extremes of metabolic behaviour as described by the Goldilocks/Lagom principle (Leese et al., 2019) and our analysis may have failed to account for this in comparing to euploid embryos.

Conclusions

We have shown that significant metabolic differences exist between euploid and aneuploid embryos which can be detected by FLIM. This preliminary data provide evidence that FLIM could be a useful non-invasive clinical tool to aid in embryo selection. Further data are needed to elucidate the causal relationship between ploidy status and metabolism. Future studies are planned to determine if metabolic signatures with FLIM can assist in embryo selection and how this correlates with pregnancy outcomes.

Supplementary data

Supplementary data are available at *Human Reproduction* online.

Data availability

The data underlying this article will be shared on reasonable request to the corresponding author.

Acknowledgements

We would like to acknowledge Becker and Hickl GmbH and Boston Electronics for the loan of electronic equipment for this research. We also acknowledge Dr Emily Seidler for her efforts with the IRB.

Authors' roles

All authors contributed to the conceptualization of the idea and experiment, critical revision of the manuscript and approval of the final draft of the manuscript. J.S.S. and M.V. also contributed to data acquisition and data interpretation. M.V. performed the analysis and J.S.S. drafted the manuscript.

Funding

The study was supported by the Blavatnik Biomedical Accelerator Grant at Harvard University. Becker and Hickl GmbH and Boston Electronics sponsored research with the loan of equipment for FLIM.

Conflict of interest

D.J.N. is an inventor on patent US20170039415A1. There are no other conflicts of interest to declare.

References

Afnan MAM, Liu Y, Conitzer V, Rudin C, Mishra A, Savulescu J, Afnan M. Interpretable, not black-box, artificial intelligence should be used for embryo selection. *Hum Reprod Open* 2021;**2021**: hoab040. doi: 10.1093/hropen/hoab040.

Ahlström A, Westin C, Reismer E, Wikland M, Hardarson T. Trophectoderm morphology: an important parameter for predicting live birth after single blastocyst transfer. *Hum Reprod* 2011;**26**: 3289–3296.

Armstrong S, Vail A, Mastenbroek S, Jordan V, Farquhar C. Time-lapse in the IVF-lab: how should we assess potential benefit? *Hum Reprod* 2015;**30**:3–8.

Becker W. Fluorescence lifetime imaging—techniques and applications. *J Microsc* 2012;**247**:119–136.

Capalbo A, Poli M, Rienzi L, Girardi L, Patassini C, Fabiani M, Cimadomo D, Benini F, Farcomeni A, Cuzzi J, *et al*. Mosaic human preimplantation embryos and their developmental potential in a prospective, non-selection clinical trial. *Am J Hum Genet* 2021;**108**: 2238–2247.

Capalbo A, Rienzi L, Cimadomo D, Maggiulli R, Elliott T, Wright G, Nagy ZP, Ubaldi FM. Correlation between standard blastocyst morphology, euploidy and implantation: an observational study in two centers involving 956 screened blastocysts. *Hum Reprod* 2014; **29**:1173–1181.

Capalbo A, Ubaldi FM, Rienzi L, Scott R, Treff N. Detecting mosaicism in trophectodermbiopsies: current challenges and future possibilities. *Hum Reprod* 2016;**32**:492–498.

Chuang TH, Hsieh JY, Lee MJ, Lai HH, Hsieh CL, Wang HL, Chang YJ, Chen SU. Concordance between different trophectoderm biopsy sites and the inner cell mass of chromosomal composition measured with a next-generation sequencing platform. *Mol Hum Reprod* 2018;**24**:593–601.

Diez-Juan A, Rubio C, Marin C, Martinez S, Al-Asmar N, Riboldi M, Díaz-Gimeno P, Valbuena D, Simón C. Mitochondrial DNA content as a viability score in human euploid embryos: less is better. *Fertil Steril* 2015;**104**:534–541.e1.

Fernandez EI, Ferreira AS, Cecílio MHM, Chéles DS, Souza R. D, Nogueira MFG, Rocha JC. Artificial intelligence in the IVF laboratory: overview through the application of different types of algorithms for the classification of reproductive data. *J Assist Reprod Genet* 2020;**37**:2359–2376.

Fragouli E, McCaffrey C, Ravichandran K, Spath K, Grifo JA, Munné S, Wells D. Clinical implications of mitochondrial DNA quantification on pregnancy outcomes: a blinded prospective non-selection study. *Hum Reprod* 2017;**32**:2340–2347.

Fragouli E, Spath K, Alfarawati S, Kaper F, Craig A, Michel CE, Kokocinski F, Cohen J, Munne S, Wells D. Altered levels of mitochondrial DNA are associated with female age, aneuploidy, and provide an independent measure of embryonic implantation potential. *PLoS Genet* 2015;**11**:e1005241.

Gardner DK, Lane M, Stevens J, Schlenker T, Schoolcraft WB. Blastocyst score affects implantation and pregnancy outcome: towards a single blastocyst transfer. *Fertil Steril* 2000a;**73**:1155–1158.

Gardner DK, Pool TB, Lane M. Embryo nutrition and energy metabolism and its relationship to embryo growth, differentiation, and viability. *Semin Reprod Med* 2000b;**18**:205–218.

Gardner DK, Wale PL, Collins R, Lane M. Glucose consumption of single post-compaction human embryos is predictive of embryo sex and live birth outcome. *Hum Reprod* 2011;**26**:1981–1986.

Ghukasyan VV, Heikal AA. *Natural Biomarkers for Cellular Metabolism: Biology, Techniques, and Applications*. Florida, USA: CRC Press, 2014.

Gleicher N, Vidali A, Braverman J, Kushnir VA, Barad DH, Hudson C, Wu YG, Wang Q, Zhang L, Albertini DF; the International PGS Consortium Study Group. Accuracy of preimplantation genetic screening (PGS) is compromised by degree of mosaicism of human embryos. *Reprod Biol Endocrinol* 2016;**14**:7.

Goodman LR, Goldberg J, Falcone T, Austin C, Desai N. Does the addition of time-lapse morphokinetics in the selection of embryos for transfer improve pregnancy rates? A randomized controlled trial. *Fertil Steril* 2016;**105**:275–285.e10.

Hardarson T, Ahlström A, Rogberg L, Botros L, Hillensjö T, Westlander G, Sakkas D, Wikland M. Non-invasive metabolomic profiling of Day 2 and 5 embryo culture medium: a prospective randomized trial. *Hum Reprod* 2012;**27**:89–96.

Hashimoto S, Morimoto N, Yamanaka M, Matsumoto H, Yamochi T, Goto H, Inoue M, Nakaoka Y, Shibahara H, Morimoto Y. Quantitative and qualitative changes of mitochondria in human preimplantation embryos. *J Assist Reprod Genet* 2017;**34**:573–580.

Hill MJ, Richter KS, Heitmann RJ, Graham JR, Tucker MJ, Decherney AH, Browne PE, Levens ED. Trophectoderm grade predicts outcomes of single-blastocyst transfers. *Fertil Steril* 2013;**99**: 1283–1289.e1.

Ho JR, Arrach N, Rhodes-Long K, Salem W, McGinnis LK, Chung K, Bendikson KA, Paulson RJ, Ahmady A. Blastulation timing is associated with differential mitochondrial content in euploid embryos. *J Assist Reprod Genet* 2018;**35**:711–720.

Irani M, Reichman D, Robles A, Melnick A, Davis O, Zaninovic N, Xu K, Rosenwaks Z. Morphologic grading of euploid blastocysts influences implantation and ongoing pregnancy rates. *Fertil Steril* 2017;**107**:664–670.

Leahy BD, Jang W-D, Yang HY, Struyven R, Wei D, Sun Z, Lee KR, Royston C, Cam L, Kalma Y *et al*. Automated measurements of key morphological features of human embryos for IVF. *Med Image Comput Comput Assist Interv* 2020;**12265**:25–35.

Leese HJ. Quiet please, do not disturb: a hypothesis of embryo metabolism and viability. *BioEssays* 2002;**24**:845–849.

Leese HJ, Sathyapalan T, Allgar V, Brison DR, Sturmey R. Going to extremes: the Goldilocks/Lagom principle and data distribution. *BMJ Open* 2019;**9**:e027767.

Leese HJ, Sturmey RG, Baumann CG, McEvoy TG. Embryo viability and metabolism: obeying the quiet rules. *Hum Reprod* 2007;**22**: 3047–3050.

Liang B, Gao Y, Xu J, Song Y, Xuan L, Shi T, Wang N, Hou Z, Zhao YL, Huang WE *et al*. Raman profiling of embryo culture medium to identify aneuploid and euploid embryos. *Fertil Steril* 2019;**111**: 753–762.e1.

Ma N, Mochel N. D, Pham PD, Yoo TY, Cho KWY, Digman MA. Label-free assessment of pre-implantation embryo quality by the fluorescence lifetime imaging microscopy (FLIM)-phasor approach. *Sci Rep* 2019;**9**:1–13.

McReynolds S, Vanderlinden L, Stevens J, Hansen K, Schoolcraft WB, Katz-Jaffe MG. Lipocalin-1: a potential marker for noninvasive aneuploidy screening. *Fertil Steril* 2011;**95**:2631–2633.

Morimoto N, Hashimoto S, Yamanaka M, Nakano T, Satoh M, Nakaoka Y, Iwata H, Fukui A, Morimoto Y, Shibahara H. Mitochondrial oxygen consumption rate of human embryos declines with maternal age. *J Assist Reprod Genet* 2020;**37**: 1815–1821.

Muller B, Lewis N, Adeniyi T, Leese HJ, Brison DR, Sturmey RG. Application of extracellular flux analysis for determining mitochondrial function in mammalian oocytes and early embryos. *Sci Rep* 2019;**9**:14.

Munné S, Kaplan B, Frattarelli JL, Child T, Nakhuda G, Shamma FN, Silverberg K, Kalista T, Handyside AH, Katz-Jaffe M *et al.*; STAR Study Group. Preimplantation genetic testing for aneuploidy versus morphology as selection criteria for single frozen-thawed embryo transfer in good-prognosis patients: a multicenter randomized clinical trial. *Fertil Steril* 2019;**112**:1071–1079.e7.

Murphy LA, Seidler EA, Vaughan DA, Resetkova N, Penzias AS, Toth TL, Thornton KL, Sakkas D. To test or not to test? A framework for counselling patients on preimplantation genetic testing for aneuploidy (PGT-A). *Hum Reprod* 2019;**34**:268–275.

Nohales-Córcoles M, Sevillano-Almerich G, Emidio GD, Tatone C, Cobo AC, Dumollard R, Los Santos Molina MD. Impact of vitrification on the mitochondrial activity and redox homeostasis of human oocyte. *Hum Reprod* 2016;**31**:1850–1858.

Pais RJ, Sharara F, Zmuidinaite R, Butler S, Keshavarz S, Iles R. Bioinformatic identification of euploid and aneuploid embryo secretome signatures in IVF culture media based on MALDI-ToF mass spectrometry. *J Assist Reprod Genet* 2020;**37**:2189–2198.

Patrizio P, Shoham G, Shoham Z, Leong M, Barad DH, Gleicher N. Worldwide live births following the transfer of chromosomally "Abnormal" embryos after PGT/A: results of a worldwide web-based survey. *J Assist Reprod Genet* 2019;**36**:1599–1607.

Popovic M, Dhaenens L, Taelman J, Dheedene A, Bialecka M, Sutter PD, Chuva De Sousa Lopes SM, Menten B, Heindryckx B. Extended in vitro culture of human embryos demonstrates the complex nature of diagnosing chromosomal mosaicism from a single trophectoderm biopsy. *Hum Reprod* 2019;**34**:758–769.

Practice Committee and Genetic Counseling Professional Group (GCPG) of the American Society for Reproductive Medicine. Clinical management of mosaic results from preimplantation genetic testing for aneuploidy (PGT-A) of blastocysts: a committee opinion. *Fertil Steril* 2020;**114**:246–254.

Practice Committees of the American Society for Reproductive Medicine and the Society for Assisted Reproductive Technology. The use of preimplantation genetic testing for aneuploidy (PGT-A): a committee opinion. *Fertil Steril* 2018;**109**:429–436.

Rubio C, Navarro-Sánchez L, García-Pascual CM, Ocali O, Cimadomo D, Venier W, Barroso G, Kopcow L, Bahçeci M, Kulmann MIR *et al*. Multicenter prospective study of concordance between embryonic cell-free DNA and trophectoderm biopsies from 1301 human blastocysts. *Am J Obstet Gynecol* 2020;**223**: 751.e1–751.e13.

Sanchez T, Venturas M, Aghvami SA, Yang X, Fraden S, Sakkas D, Needleman DJ. Combined noninvasive metabolic and spindle imaging as potential tools for embryo and oocyte assessment. *Hum Reprod* 2019;**34**:2349–2361.

Sanchez T, Wang T, Pedro MV, Zhang M, Esencan E, Sakkas D, Needleman D, Seli E. Metabolic imaging with the use of fluorescence lifetime imaging microscopy (FLIM) accurately detects mitochondrial dysfunction in mouse oocytes. *Fertil Steril* 2018;**110**: 1387–1397.

Schoolcraft WB, Gardner DK, Lane M, Schlenker T, Hamilton F, Meldrum DR. Blastocyst culture and transfer: analysis of results and parameters affecting outcome in two in vitro fertilization programs. *Fertil Steril* 1999;**72**:604–609.

Scott RT, Upham KM, Forman EJ, Hong KH, Scott KL, Taylor D, Tao X, Treff NR. Blastocyst biopsy with comprehensive chromosome screening and fresh embryo transfer significantly increases in vitro fertilization implantation and delivery rates: a randomized controlled trial. *Fertil Steril* 2013;**100**:697–703.

Seidler EA, Sanchez T, Venturas M, Sakkas D, Needleman DJ. Noninvasive imaging of mouse embryo metabolism in response to induced hypoxia. *J Assist Reprod Genet* 2020;**37**:1797–1805.

Seli E, Vergouw CG, Morita H, Botros L, Roos P, Lambalk CB, Yamashita N, Kato O, Sakkas D. Noninvasive metabolomic profiling as an adjunct to morphology for noninvasive embryo assessment in women undergoing single embryo transfer. *Fertil Steril* 2010;**94**:535–542.

Shear MA, Vaughan DA, Modest AM, Seidler EA, Leung AQ, Hacker MR, Sakkas D, Penzias AS. Blasts from the past: is morphology useful in PGT-A tested and untested frozen embryo transfers? *Reprod Biomed Online* 2020;**41**:981–989.

Simopoulou M, Sfakianoudis K, Maziotis E, Antoniou N, Rapani A, Anifandis G, Bakas P, Bolaris S, Pantou A, Pantos K *et al*. Are computational applications the "crystal ball" in the IVF laboratory? The evolution from mathematics to artificial intelligence. *J Assist Reprod Genet* 2018;**35**:1545–1557.

Snijder TAB, Bosker RJ. *Multilevel Analysis: An Introduction to Base and Advance Multilevel Modeling*. London: Sage, 2011.

Stecher A, Vanderzwalmen P, Zintz M, Wirleitner B, Schuff M, Spitzer D, Zech NH. Transfer of blastocysts with deviant morphological and morphokinetic parameters at early stages of in-vitro development: a case series. *Reprod Biomed Online* 2014;**28**:424–435.

Sutton-Mcdowall ML, Gosnell M, Anwer AG, White M, Purdey M, Abell AD, Goldys EM, Thompson JG. Hyperspectral microscopy can detect metabolic heterogeneity within bovine post-compaction embryos incubated under two oxygen concentrations (7% versus 20%). *Hum Reprod* 2017;**32**:2016–2025.

Tan TCY, Mahbub SB, Campugan CA, Campbell JM, Habibalahi A, Chow DJX, Mustafa S, Goldys EM, Dunning KR. Non-invasive, label-free optical analysis to detect aneuploidy within the inner cell

mass of the preimplantation embryo. *bioRxiv* 2020;1–49. doi: 10.1101/2020.11.01.364133.

Tao X, Landis JN, Krisher RL, Duncan FE, Silva E, Lonczak A, Scott RT, Zhan Y, Chu T, Scott RT *et al.* Mitochondrial DNA content is associated with ploidy status, maternal age, and oocyte maturation methods in mouse blastocysts. *J Assist Reprod Genet* 2017;**34**: 1587–1594.

Tran D, Cooke S, Illingworth PJ, Gardner DK. Deep learning as a predictive tool for fetal heart pregnancy following time-lapse incubation and blastocyst transfer. *Hum Reprod* 2019;**34**: 1011–1018.

Treff NR, Zhan Y, Tao X, Olcha M, Han M, Rajchel J, Morrison L, Morin SJ, Scott RT. Levels of trophectoderm mitochondrial DNA do not predict the reproductive potential of sibling embryos. *Hum Reprod* 2017;**32**:954–962.

Van Den Abbeel E, Balaban B, Ziebe S, Lundin K, Cuesta MJG, Klein BM, Helmgaard L, Arce JC. Association between blastocyst morphology and outcome of single-blastocyst transfer. *Reprod Biomed Online* 2013;**27**:353–361.

Venturas M, Shah JS, Yang X, Sanchez TH, Conway W, Sakkas D, Needleman DJ. Metabolic state of human blastocysts measured by fluorescence lifetime imaging microscopy. *Hum Reprod* 2022; deab283. doi:10.1093/humrep/deab283.

Vergouw CG, Kieslinger DC, Kostelijk EH, Botros LL, Schats R, Hompes PG, Sakkas D, Lambalk CB. Day 3 embryo selection by metabolomic profiling of culture medium with near-infrared spectroscopy as an adjunct to morphology: A randomized controlled trial. *Hum Reprod* 2012;**27**:2304–2311.

VerMilyea M, Hall JMM, Diakiw SM, Johnston A, Nguyen T, Perugini D, Miller A, Picou A, Murphy AP, Perugini M. Development of an artificial intelligence-based assessment model for prediction of embryo viability using static images captured by optical light microscopy during IVF. *Hum Reprod* 2020;**35**:770–784.

Victor AR, Griffin DK, Brake AJ, Tyndall JC, Murphy AE, Lepkowsky LT, Lal A, Zouves CG, Barnes FL, McCoy RC *et al.* Assessment of aneuploidy concordance between clinical trophectoderm biopsy and blastocyst. *Hum Reprod* 2019;**34**:181–192.

Wong KM, Repping S, Mastenbroek S. Limitations of embryo selection methods. *Semin Reprod Med* 2014;**32**:127–133.

Yamanaka M, Hashimoto S, Amo A, Ito-Sasaki T, Abe H, Morimoto Y. Developmental assessment of human vitrified-warmed blastocysts based on oxygen consumption. *Hum Reprod* 2011;**26**: 3366–3371.

Yang L, Cai S, Zhang S, Kong X, Gu Y, Lu C, Dai J, Gong F, Lu G, Lin G. Single embryo transfer by Day 3 time-lapse selection versus Day 5 conventional morphological selection: a randomized, open-label, non-inferiority trial. *Hum Reprod* 2018;**33**:869–876.

Yang X, Ha G, Needleman D. A coarse-grained NADH redox model enables inference of subcellular metabolic fluxes from fluorescence lifetime imaging. *Elife* 2021;**10**:e73808. doi:10.7554/eLife.73808.